ARMY RESEARCH LABORATORY

# Road Navigation by a Passive Millimeter-Wave Imager Mounted on an Aircraft

by Joseph D. Silverstein

ARL-TR-3017 July 2003

Approved for public release; distribution unlimited.

20030806 003

## NOTICES

### Disclaimers

The findings in this report are not to be construed as an official Department of the Army position, unless so designated by other authorized documents.

Citation of manufacturers' or trade names does not constitute an official endorsement or approval of the use thereof.

**Army Research Laboratory**
Adelphi, MD 20783-1197

**ARL-TR-3017** **July 2003**

# Road Navigation by a Passive Millimeter-Wave Imager Mounted on an Aircraft

**Joseph D. Silverstein**
**Sensors and Electron Devices Directorate, ARL**

**Approved for public release; distribution unlimited.**

# REPORT DOCUMENTATION PAGE

*Form Approved*
*OMB No. 0704-0188*

Public reporting burden for this collection of information is estimated to average 1 hour per response, including the time for reviewing instructions, searching existing data sources, gathering and maintaining the data needed, and completing and reviewing the collection information. Send comments regarding this burden estimate or any other aspect of this collection of information, including suggestions for reducing the burden, to Department of Defense, Washington Headquarters Services, Directorate for Information Operations and Reports (0704-0188), 1215 Jefferson Davis Highway, Suite 1204, Arlington, VA 22202-4302. Respondents should be aware that notwithstanding any other provision of law, no person shall be subject to any penalty for failing to comply with a collection of information if it does not display a currently valid OMB control number.
PLEASE DO NOT RETURN YOUR FORM TO THE ABOVE ADDRESS.

| 1. REPORT DATE *(DD-MM-YYYY)* | 2. REPORT TYPE | 3. DATES COVERED (From - To) |
|---|---|---|
| July 2003 | Final | FY02 to FY03 |

**4. TITLE AND SUBTITLE**
Road Navigation by a Passive Millimeter-Wave Imager Mounted on an Aircraft

**5a. CONTRACT NUMBER**

**5b. GRANT NUMBER**

**5c. PROGRAM ELEMENT NUMBER**

**6. AUTHOR(S)**
Joseph D. Silverstein

**5d. PROJECT NUMBER**
3NE3HH

**5e. TASK NUMBER**

**5f. WORK UNIT NUMBER**

**7. PERFORMING ORGANIZATION NAME(S) AND ADDRESS(ES)**
U.S. Army Research Laboratory
Attn: AMSRL-SE-RM
2800 Powder Mill Road
Adelphi, MD 20783-1197

**8. PERFORMING ORGANIZATION REPORT NUMBER**
ARL-TR-3017

**9. SPONSORING/MONITORING AGENCY NAME(S) AND ADDRESS(ES)**
U.S. Army Research Laboratory
2800 Powder Mill Road
Adelphi, MD 20783-1197

**10. SPONSOR/MONITOR'S ACRONYM(S)**

**11. SPONSOR/MONITOR'S REPORT NUMBER(S)**

**12. DISTRIBUTION/AVAILABILITY STATEMENT**
Approved for public release; distribution unlimited.

**13. SUPPLEMENTARY NOTES**

**14. ABSTRACT**

Simulations are carried out of the generation and integration of passive millimeter-wave (PMMW) digital video images of a simple scene consisting of a road bordered on either side by vegetation growth. The MMW road and growth brightness temperatures, their standard deviations, and the parameters of the simulated PMMW imaging system are based on realistic values. It is assumed that the simulated PMMW sensor is mounted on a low-flying aircraft. The processing consists only of straightforward integration of all or parts of consecutive video image frames. In the simulations the difference between the vegetation growth and road average brightness temperatures could have values from 1 K thru 15 K. The variation in the vegetation growth or road brightness temperature due only to terrain non-uniformities could have values from 0 K thru 2 K. Variations due only to system thermal noise could have values from 3 K thru 15 K. The number of consecutive frames integrated could be 2 thru 31. These simulations show that road navigation is possible for at least some combinations of the terrain and thermal noise brightness temperature variations studied, if the vegetation growth-to-road, average brightness temperature difference is 2 K or larger, and 31 consecutive frames or less are integrated. However, in order to accomplish road navigation when that brightness temperature difference is only 1 K, and for any of the combinations of terrain and thermal noise brightness temperature variations studied, more than 31 consecutive frames would have to be integrated. The simulations also show that, for fixed values of all the brightness temperature parameters, and for a given angular separation between consecutive brightness temperature measurements, if the antenna aperture size could be increased over that currently feasible for airborne PMMW imaging systems, the number of frames that would need to be integrated to achieve a given degree of vegetation growth-to-road brightness temperature contrast would be decreased.

**15. SUBJECT TERMS**
Millimeter-wave, video image processing, video frame, frame rate

| 16. SECURITY CLASSIFICATION OF: | | | 17. LIMITATION OF ABSTRACT | 18. NUMBER OF PAGES | 19a. NAME OF RESPONSIBLE PERSON |
|---|---|---|---|---|---|
| a. REPORT | b. ABSTRACT | c. THIS PAGE | | | Joseph D. Silverstein |
| UNCLASSIFIED | UNCLASSIFIED | UNCLASSIFIED | UL | | 19b. TELEPHONE NUMBER *(Include area code)* (301) 394-3170 |

**Standard Form 298 (Rev. 8/98)**
Prescribed by ANSI Std. Z39.18

## Contents

**List of Figures** iv

**List of Tables** vi

**1. Introduction** 1

**2. Simulation Parameters and Methodology** 1

2a. Scene simulation....1

2b. Method of single frame "simulation"....4

2c. Point spread function distortion....4

2d. Thermal noise addition....4

**3. Frame Integration** 5

3a. Frame rows and columns....5

3b. Partially integrated frame formation....5

3c. *dx*-column integrated frame formation....7

3d. Formation of the fully integrated frame....9

**4. Simulation Steps** 10

**5. Simulation Results** 11

5a. Frame images and plots....11

5b. Contrast figure of merit....13

5c. Road distinguishability....19

**6. Generation of Video Frames** 23

**7. Conclusions** 25

**References** 26

## List of Figures

Figure 1. Schematics of a simulated scene (1a) and a frame (1b). The growth and road patches of the scene and frame each have 10 brightness temperature pixels "cross track," for a total of 30, and a sufficient number of brightness temperature pixels "along track" to extract the desired number of frames for the simulation. Each frame to be extracted has 30 "cross track" brightness temperature pixels, and 63 "along track" brightness temperature pixels. Each frame is delayed relative to the preceding frame by the time needed by the imaging system to measure 2 samples "along track" ..... 3

Figure 2. Formation of a 25-column, partially integrated frame by integrating portions of consecutive, single frame numbers 1–20, where "column" refers to brightness temperature pixels at the same "along track" position of the scene. The partially integrated frame results from the averaging of the 20 independent brightness temperature values, contained in each of the pixels ("cross track," "along track" location) of columns 39–63 of the scene. These pixels are in columns 39–63 of single frame 1, columns 37–61 of single frame 2, columns 35–59 of single frame 3, and so on, down to columns 1–25 of single frame 20. These 20, 25-column single frame slices are averaged to form columns 1–25 of the 63-column, fully integrated from being formed ..... 6

Figure 3. Formation of *dx*(2)column, integrated frame resulting from integrating 20 frames, where "column" refers to all pixels at the same "along track" position of the scene. This *dx*-column integrated frame results from the averaging of 20 independent brightness temperature measurements, contained in single frames 2–21, in each of the pixels ("cross track," "along track" locations) in columns 64 and 65 of the scene. These pixels are in columns 62 and 63 of single frame 2, columns 60 and 61 of single frame 3, columns 58 and 59 of single frame 4, and so on, down to columns 24 and 25 of single frame 21. These 20, 2-column, frame slices are averaged to form columns 26 and 27 of the 63-column, fully integrated frame being formed. Corresponding procedures are carried out to form the fully integrated frame's columns 28 and 29, 30 and 31, 32 and 33, and so on, down to columns 62 and 63 ..... 8

Figure 4. Concatenation of one, 25-column slice formed by integrating 25-column portions of frames 1–20, where "column" refers to all brightness temperature pixels at the same "along track" position of the scene, (see Figure 2), and 19, 2-column slices, each formed by integrating 2-column portions of frames 2–21, frames 3–22, frames 4–23, and so on, down to frames 20–39 (see Figure 3). The result is a fully integrated, 63-column frame..... 9

Figure 5. Images of a single and processed frame with a road (center patch) average brightness temperature of 270 K, a growth (upper and lower patches) average brightness temperature and a thermal noise minimum resolvable brightness temperature difference of 10 K. The psf is appropriate for a PMMW imaging system at 84.5 GHz oversampling the scene by ×2. 5a. A simulated, single frame that has terrain variation noise only. 5b. The simulated, single frame that results from convolving the frame in 5a with the psf and adding thermal noise. 5c. The fully integrated frame arising from the integration of 20 consecutive, single frames, such as the one in 5b, in the manner illustrated in Figures 1–4..... 12

Figure 6. Plots of brightness temperature at "along track" position 32 vs. "cross track" position in a frame having only terrain variation, in a frame having both terrain variation and thermal noise, as well as distortion from the psf, and the processed frame arising from the integration of 20 frames. The road average brightness temperature is 270 K, the growth average brightness temperature is 275 K, the terrain variation minimum resolvable brightness temperature difference is 1K, the thermal noise minimum resolvable brightness temperature difference is 10 K, and the psf is appropriate for a PMMW imaging system that oversamples the scene by ×2. The 20-frame integration processes illustrated in Figures 1–4 ..... 13

Figure 7. Contrast-to-noise ratio vs. number of frames integrated for the fully integrated frame based on the central limit theorem (CLT), and as generated by simulations with blurring by a point spread function for an oversampling of ×2, and without blurring. The vegetation growth-to-road brightness temperature difference is 5 K, the terrain variation minimum resolvable brightness temperature difference is 1 K, and the thermal noise minimum resolvable brightness temperature difference is 3 K ..... 15

Figure 8. Contrast-to-noise ratio vs. number of frames integrated for the fully integrated frame based on the central limit theorem (CLT), and as generated by simulations with blurring by a point spread function for an oversampling of ×2, and without blurring. The vegetation growth-to-road brightness temperature difference is 5 K, the terrain variation minimum resolvable brightness temperature difference is 1 K, and the thermal noise minimum resolvable brightness temperature difference is 5 K ..... 16

Figure 9. Contrast-to-noise ratio vs. number of frames integrated for the fully integrated frame based on the central limit theorem (CLT), and as generated by simulations with blurring by a point spread function for an oversampling of ×2, and without blurring. The vegetation growth-to-road brightness temperature difference is 5 K, the terrain variation minimum resolvable brightness temperature difference is 1 K, and the thermal noise minimum resolvable brightness temperature difference is 10 K ..... 17

Figure 10. Contrast-to-noise ratio vs. number of frames integrated for the fully integrated frame based on the central limit theorem (CLT), and as generated by simulations with blurring by a point spread function for an oversampling of ×2, and without blurring. The vegetation growth-to-road brightness temperature difference is 5 K, the terrain variation minimum resolvable brightness temperature difference is 1 K, and the thermal noise minimum resolvable brightness temperature difference is 15 K ..... 18

Figure 11. Brightness temperature contrast-to-noise ratio vs. number of frames integrated for the fully integrated frame based on the central limit theorem (CLT), and as generated by simulations without blurring as well as with blurring by point spread functions for oversamplings of ×1 (aperture diameter = 116 cm), ×2 (aperture diameter = 58 cm), and ×4 (aperture diameter = 29 cm). The vegetation growth-to-road brightness temperature difference is 5 K, the terrain variation minimum resolvable brightness temperature difference is 1 K, and the thermal noise minimum resolvable brightness temperature difference is 10 K ..... 19

Figure 12. Fully integrated frames resulting in brightness temperature contrast-to-noise ratios of 0 dB (12a), 1 dB (12b), and 2 dB (12c) for a vegetation growth-to-road brightness temperature difference of 5 K, a terrain variation minimum resolvable brightness temperature difference of 1 K, and a thermal noise minimum resolvable brightness temperature difference of 0 K ..... 20

## List of Tables

Table 1a. Platform parameters ..... 2

Table 1b. Imaging System and Frame Simulation Parameters ..... 2

Table 2a. Minimum required number of frames that must be integrated to achieve specified values of contrast-to-noise ratio (*cnr)* for vegetation growth-to-road brightness temperature differences of 1 K and 2 K ..... 21

Table 2b. Minimum required number of frames that must be integrated to achieve specified values of contrast-to-noise ratio (*cnr)* for a vegetation growth-to-road brightness temperature difference of 5 K ..... 22

Table 2c. Minimum required number of frames that must be integrated to achieve specified values of contrast-to-noise ratio (*cnr)* for a vegetation growth-to-road brightness temperature difference of 10 K ..... 22

Table 2d. Minimum required number of frames that must be integrated to achieve specified values of contrast-to-noise ratio (*cnr)* for a vegetation growth-to-road brightness temperature difference of 15 K ..... 23

Table 3. Range of the frame numbers of the 39, consecutive single frames involved in forming each of the first 10, fully integrated frames. The fully integrated frames are formed by integrating portions of 20 consecutive, single frames from among those 39 consecutive, single frames. For each fully integrated frame number the table also gives the range of the column numbers of the scene columns imaged by those fully integrated frames. The number of columns in both the single and fully integrated frames is 63, and the frame-to-frame delay in "along track" brightness temperature pixels is 2 ..... 24

# 1. Introduction

It is well known that passive millimeter-wave (PMMW) imaging systems can operate in limited visibility conditions during day and night when other sensors have limited performance *(1)*. This paper suggests that it may be feasible for an aircraft to navigate along a road, even in limited visibility conditions, by means of a PMMW imaging sensor. Moreover, this method is even effective when the brightness temperature of the road does not differ significantly from that of its surroundings. Such a small difference may occur when the road is made of a material such as dirt, asphalt, or concrete, and its surroundings consist of some higher emissivity vegetation.

PMMW sensors are attractive for road navigation by aircraft flying at a relatively low altitude, since in most such road scenarios the spatial resolution that can be achieved by the sensors should not be a limiting factor in distinguishing the road from its surroundings. Resolution improvement investigations carried out at ARL *(2)* evaluated the performance of several powerful image restoration algorithms that were designed to improve the spatial resolution in PMMW images obtained with a stationary sensor. Those investigations showed that the degree of resolution improvement is influenced by the inherent temperature contrast and noise in the original image.

The main challenge for processing PMMW video images of navigation scenes is to restore the contrast of the road to its surroundings, which is degraded by noise due to spatial variations of the terrain and by system thermal noise. This contrast may be improved by decreasing the minimum resolvable brightness temperature difference in the processed video image. The latter is proportional to the reciprocal of the square root of the sensor integration time, which, in turn, is determined by the frame rate of the system. One can effectively increase the sensor integration time for a small area of the scene, samples of whose brightness temperatures are measured by the sensor, by averaging together, or "integrating," several consecutive video image frames, each of which contains brightness temperature samples of some larger area which contains the smaller area. This paper shows that the image contrast may be significantly and efficiently increased using consecutive video frame integration.

# 2. Simulation Parameters and Methodology

## 2a. Scene simulation

Table 1a gives the airborne platform parameters used in the simulations, and Table 1b gives the MMW imaging system and frame parameters used in the simulations. These parameters were chosen to approximate those of a PMMW system currently being developed *(3)*, and to be appropriate for such a system mounted on a low-flying helicopter. From Table 1b the number of brightness temperature measurements in a video frame, henceforth to be referred to as "pixels," is 30 "cross-track" and 63 "along track." Accordingly, for simplicity, the road scene simulated was also assumed to have 30 brightness temperature samples "cross track," and a number of

brightness temperature samples "along track" that was at least sufficient to allow the "simulation" of the desired number of single frames in the manner to be described in subsection 2b.

Table 1a. Platform parameters.

| Parameter | Value |
|---|---|
| Altitude | 100 m |
| Speed | 44.7 m/sec (100 mph) |

Table 1b. Imaging System and Frame Simulation Parameters.

| Parameter | Value |
|---|---|
| Center Frequency | 84.5 GHz |
| Antenna circular aperture diameter | 58 cm |
| Angle between consecutive brightness temperature measurement positions at the imager:<br><br>"cross track"<br>"along track" | <br><br>0.38 deg<br>0.38 deg |
| Number of brightness temperature measurements in a frame image:<br><br>"cross track"<br>"along track" | <br><br>30<br>63 |
| Video frame rate | 30 Hz |
| Depression angle | 90 deg (nadir) |

Figures 1a and 1b show schematics of a typical simulated road scene and frame image, respectively. It consists of three long, straight, parallel patches at different brightness temperatures. The number of "cross-track" samples for each patch in the scene and frame was 10, yielding the total number of 30 "cross-track" samples given in Table 1b. In any simulated scene the average brightness temperature in the central patch, considered to be the road, was fixed at 270 K, while the average brightness temperature in the patches on either side, considered to be some type of vegetation growth, was varied and assumed to be 270 K + $\Delta T$, where $\Delta T$ was assigned the values 1 K, 2 K, 5 K, 10 K, and 15 K *(1,4)*. The statistical variations in the brightness temperature of both the road and growth patches can be expressed as the minimum resolvable temperature due to terrain variations, ***mrtte***. It was given the values 0 K, 1 K, or 2 K *(1,4)*. A Gaussian brightness temperature distribution having an average value of 0 K and a standard deviation equal to ***mrtte*** was added to the constant brightness temperatures of the scene before forming any frames using the simulated scene.

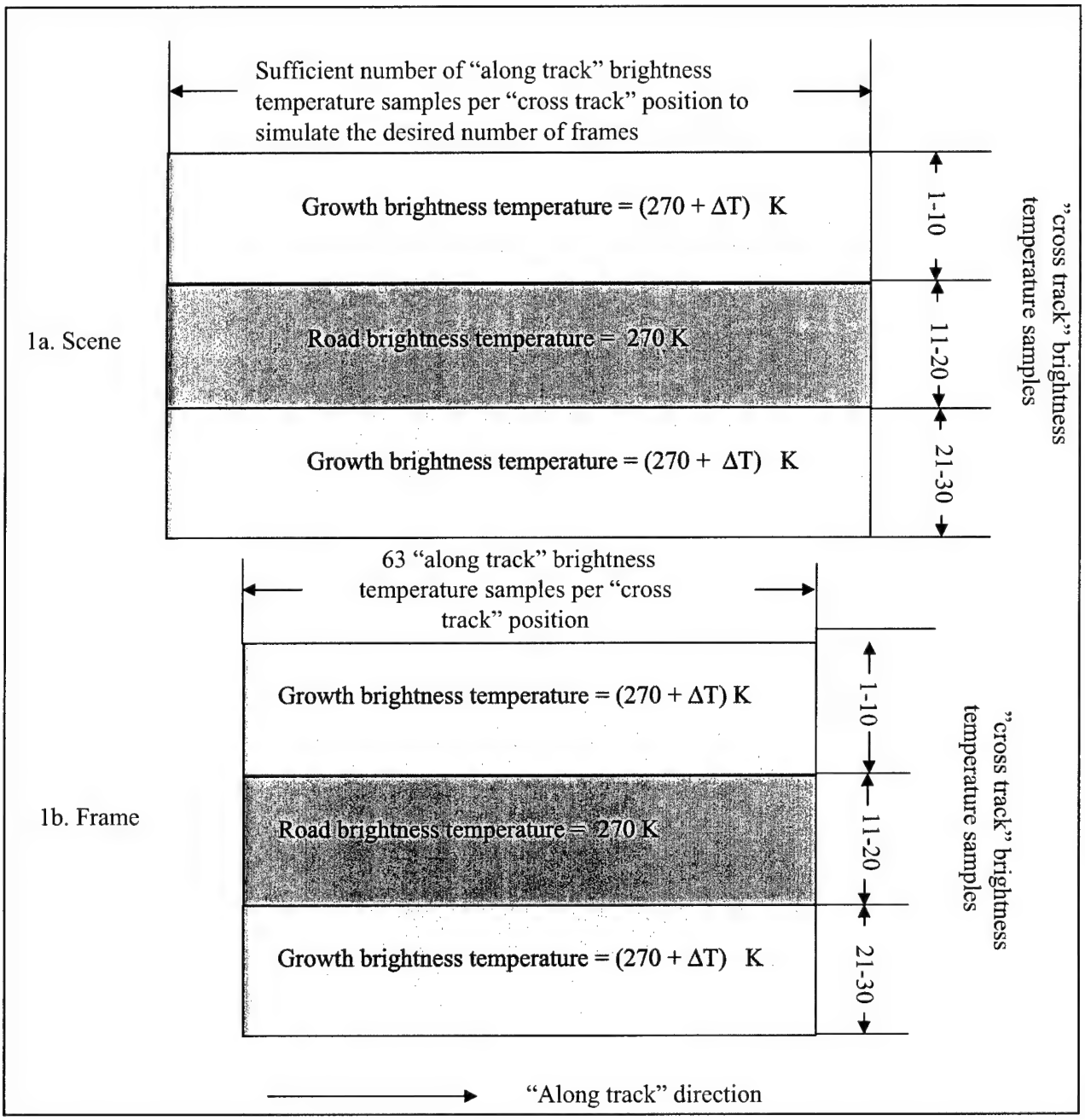


Figure 1. Schematics of a simulated scene (1a) and a frame (1b). The growth and road patches of the scene and frame each have 10 brightness temperature pixels "cross track," for a total of 30, and a sufficient number of brightness temperature pixels "along track" to extract the desired number of frames for the simulation. Each frame to be extracted has 30 "cross track" brightness temperature pixels, and 63 "along track" brightness temperature pixels. Each frame is delayed relative to the preceding frame by the time needed by the imaging system to measure 2 samples "along track."

## 2b. Method of single frame "simulation"

It is seen from Table 1b that the angle separating consecutive brightness temperature measurements, both "cross track" and "along track," and henceforth to be referred to as "pixel angle," is 0.38 deg. Thus, the field of view (FOV) of the imager is 11 deg (0.38×30) "cross track" and 24 deg (0.38×63) "along track." Based on that pixel angle and the frame rate of 30 Hz, given in Table 1b, and on the platform speed of 44.7 m/sec and platform altitude of 100 m given in Table 1a, one may infer that the number of "along track" pixels, ***dx***, of the scene by which the first pixel of a frame is delayed relative to the first pixel of the preceding frame is $(1/30)(44.7/100)(180/\pi)/0.38 = 2.25$, which, when rounded down, is 2. This "along-track", 2-pixel delay and the number of consecutive single frames that need to be simulated then uniquely determine the minimum number of "along track" pixels the simulated scene is required to have. Thus, to simulate one single frame, the scene must have 63 columns, to simulate two single frames the scene must have 65 columns, to simulate three single frames the scene must have 67 columns, and so on. Section 3d discusses the method that was used to determine the number of frames that needed to be extracted

## 2c. Point spread function distortion

From Table 1b the central frequency of the imager is 84.5 GHz, and the antenna aperture is a circle having a diameter of 58 cm. These two parameters uniquely determine the point spread function (psf), which, in turn, determines the shape of the antenna's footprint on the ground. In particular, the null-to-null angle of the central and strongest lobe of the footprint for the psf used is 0.856 deg. After a single frame is simulated using the scene, its road and growth brightness temperature profiles, which already contained variations due to ***mrtte***, were further distorted by convolving them with the psf *(2)*. It can be seen from the simulation results that the extent of the blurring increases monotonically with the oversampling, ***osamp*** *(5)*. In this paper the latter is defined as the ratio of the number of "along track," brightness temperature measurements that are made on the ground in some angular interval and the number of null-to-null angles that are on the ground in that interval. Therefore,

$$\textbf{\textit{osamp}} = \text{floor}((\text{null-to-null angle})/(\text{pixel angle})), \qquad (1)$$

where floor( ) indicates that the quantity in parentheses is rounded to the next lowest integer. With the null-to-null angle of 0.86 deg and the pixel angle in Table 1b of 0.38 deg equation 1 yields an ***osamp*** of 2. Some simulations with the same pixel angle of 0.38 deg, and with aperture diameters of 29 cm and 116 cm were also carried out, which give a twice-as-large ***osamp*** of 4 and a half-as-large ***osamp*** of 1, respectively.

## 2d. Thermal noise addition

The thermal noise of the imaging system can be expressed as the minimum resolvable brightness temperature due to thermal noise, ***mrtth***. The minimum, "state-of-the-art" value assigned to this parameter was 3 K *(3)*. It was also allowed to have the easily-attainable values 5 K, 10 K, or 15 K. After the brightness temperature profile of a frame, to which terrain variation noise had already been added, was distorted by the psf, a Gaussian brightness temperature distribution having an average value of 0 and a standard deviation equal to ***mrtth*** was added to that distorted profile. This resulted in the final form of a simulated, single frame.

## 3. Frame Integration

### 3a. Frame rows and columns

It is convenient to consider the collection of brightness temperature measurements in a frame, which is determined by the FOV of the imager (see section 2a), to be a matrix of numbers. Accordingly, in this report the word "row" is used to denote all the pixels in a frame that are at some "cross track" location, and the word "column" is used to denote all the pixels in a frame that are at some "along track" location. Thus, from Table 1b, the number, ***Nrows***, of rows in a frame is 30 and the number, ***Ncols***, of columns in a frame is 63.

In the integration process of these simulations portions of consecutive single frames are added to form two other types of frames: partially integrated frames and ***dx***-column integrated frames. The latter two types of frames are then used to form the processed, fully integrated, ***Ncols***-column, integrated frame. The method of forming partially integrated and ***dx***-column frames are discussed in subsections 3b and 3c, respectively, and the method of forming the fully integrated frame is discussed in subsection 3d.

### 3b. Partially integrated frame formation

In this report a partially integrated frame is a frame resulting from consecutive frame integration that has fewer columns than ***Ncols.*** The partially integrated frame is formed by adding the common areas of a *particular* set of ***Nframes***, consecutive, single frames. This process is illustrated in Figure 2 for the case in which ***Nframes*** = 20. Since there is a column pixel delay, ***dx***, between frames, the number of columns, ***Com_cols***, in the partially integrated frame must be

$$Com_cols = Ncols - (Nframes - 1)dx . \qquad (2)$$

As is expected, ***Com_cols*** =***Ncols*** when ***Nframes*** = 1. For the case illustrated in Figure 2, i.e. ***Nframes*** = 20 and ***dx*** = 2 , equation 2 yields ***Com_cols*** = 25. Figure 2 shows how the partially integrated frame is formed by adding columns 39-63 of single frame 1, to columns 37-61 of single frame 2, to columns 35-59 of single frame 3, and so on, down to columns 1-25 of frame 20. The fact that the frame-to-frame column pixel delay, ***d x***= 2 guarantees that each of these 25-column slices of those single frames that is involved in this integration process contains brightness temperature measurements of the same 25-column slice of the sensor's FOV.

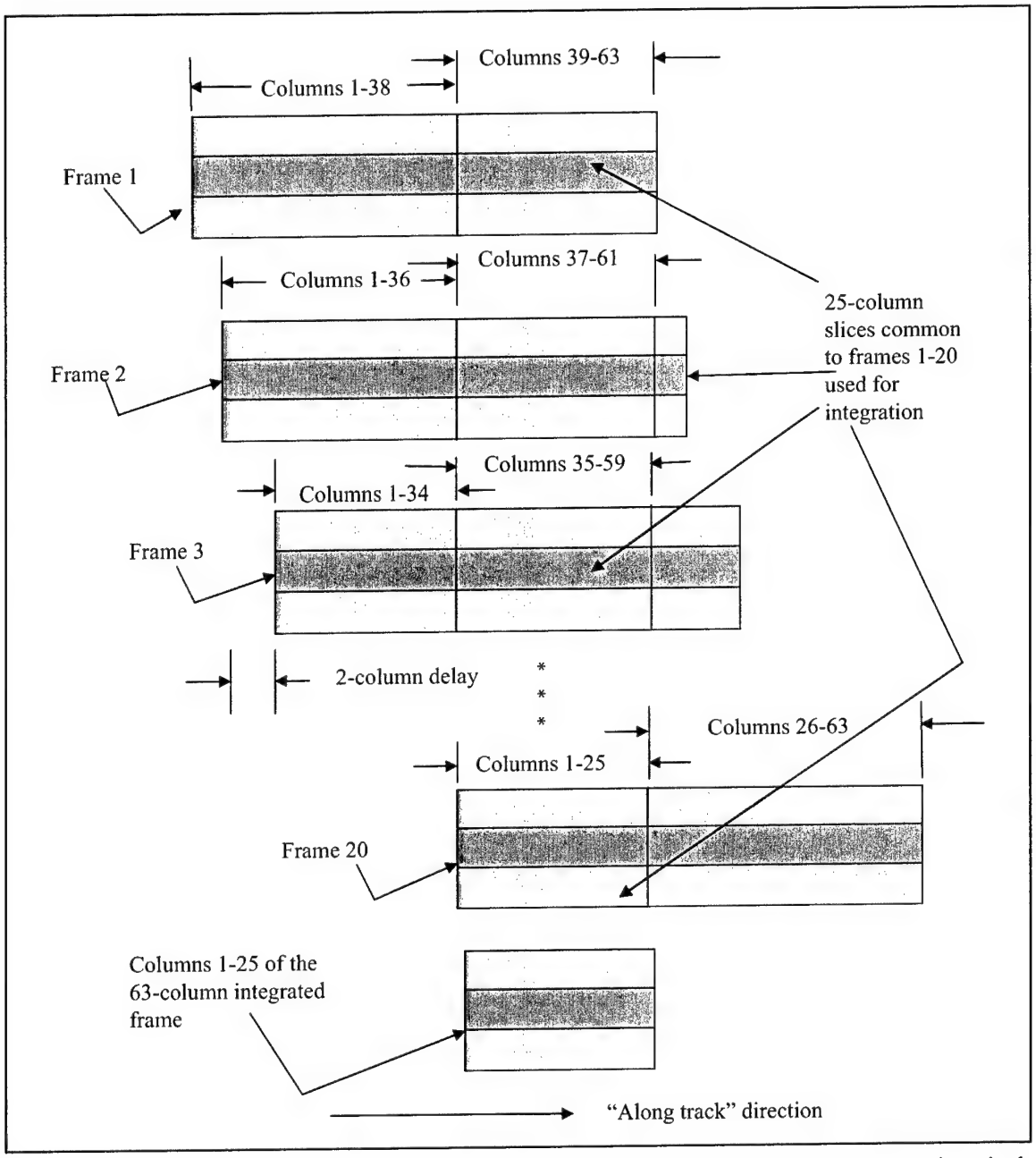


Figure 2. Formation of a 25-column, partially integrated frame by integrating portions of consecutive, single frame numbers 1–20, where "column" refers to brightness temperature pixels at the same "along track" position of the scene. The partially integrated frame results from the averaging of the 20 independent brightness temperature values, contained in each of the pixels ("cross track," "along track" location) of columns 39–63 of the scene. These pixels are in columns 39–63 of single frame 1, columns 37–61 of single frame 2, columns 35–59 of single frame 3, and so on, down to columns 1–25 of single frame 20. These 20, 25-column single frame slices are averaged to form columns 1–25 of the 63-column, fully integrated from being formed.

The maximum number of consecutive frames, ***Nframes_maxp***, for which such a partially integrated frame formation process is possible is that value of ***Nframes*** in equation 2 that yields ***Com_cols*** = 1. Thus,

$$Nframes_maxp = \text{floor}(\frac{Ncols - 1}{dx}) + 1. \quad (3)$$

In our case, in which ***Ncols*** = 63 and ***dx*** = 2, equation 3 yields ***Nframes_maxp*** = 32.

### 3c. *dx*-column integrated frame formation

As can be seen from equation 2, the number of columns of the ***Ncols***-column, fully integrated frame that remain to be formed after forming the partially integrated frame is (***Nframes***–1)***dx***. In these simulations each set of ***dx*** columns beyond the first ***Com_cols*** columns of the ***Ncols***-column, fully integrated frame is formed by adding the appropriate ***dx*** columns of a *different* set of ***Nframes*** frames. We call the result of this process a ***dx***-column integrated frame. Figure 3 illustrates this procedure for the formation of the first ***dx***(=2)-column integrated frame, which will contain the processed columns 26 and 27 of the fully integrated frame. Again, the number of frames, ***Nframes***, being integrated is 20, just as it was for the partially integrated frame formation illustrated in Figure 2. It is seen in Figure 3 that these two columns are formed by adding columns 62 and 63 of frame 2, columns 60 and 61 of frame 3, columns 58 and 59 of frame 4, and so on, down to columns 24 and 25 of frame 21. Again, the fact that the frame-to-frame column pixel delay ***dx*** = 2 guarantees that each of these 2-column frame slices contains brightness temperature measurements of the *same* 2-column slice of the scene. Moreover, from Figure 2, it is seen that the last column of frame 2 entering into the formation of the partially integrated frame is 61. It is also seen from Figure 3, that the first column of frame 2 entering into the formation of the first ***dx***-column frame is 62. It is therefore guaranteed that this first ***dx***-column frame has brightness temperature measurements of the two columns of the scene that immediately follow the 25 columns of the scene that are processed in the partially integrated frame.

In a similar manner the next two columns, 28 and 29, of the fully integrated frame are formed by adding appropriate 2-column slices of frames 3 thru 22. This procedure is repeated until all the ***Nframes***(=20) −1 = 19, ***dx***(=2)-column integrated frames that are required are formed.

The maximum number of consecutive frames, ***Nframes_maxd***, which can enter into the formation of a ***dx***-column integrated frame is the maximum number of consecutive frames which can contain a common, ***dx***-column, slice of the scene. Clearly this number is

$$Nframes_maxd = \text{floor}(\frac{Ncols}{dx}). \quad (4)$$

In our case, in which ***Ncols*** = 63 and ***dx*** = 2, equation 4 yields ***Nframes_maxd*** = 31.

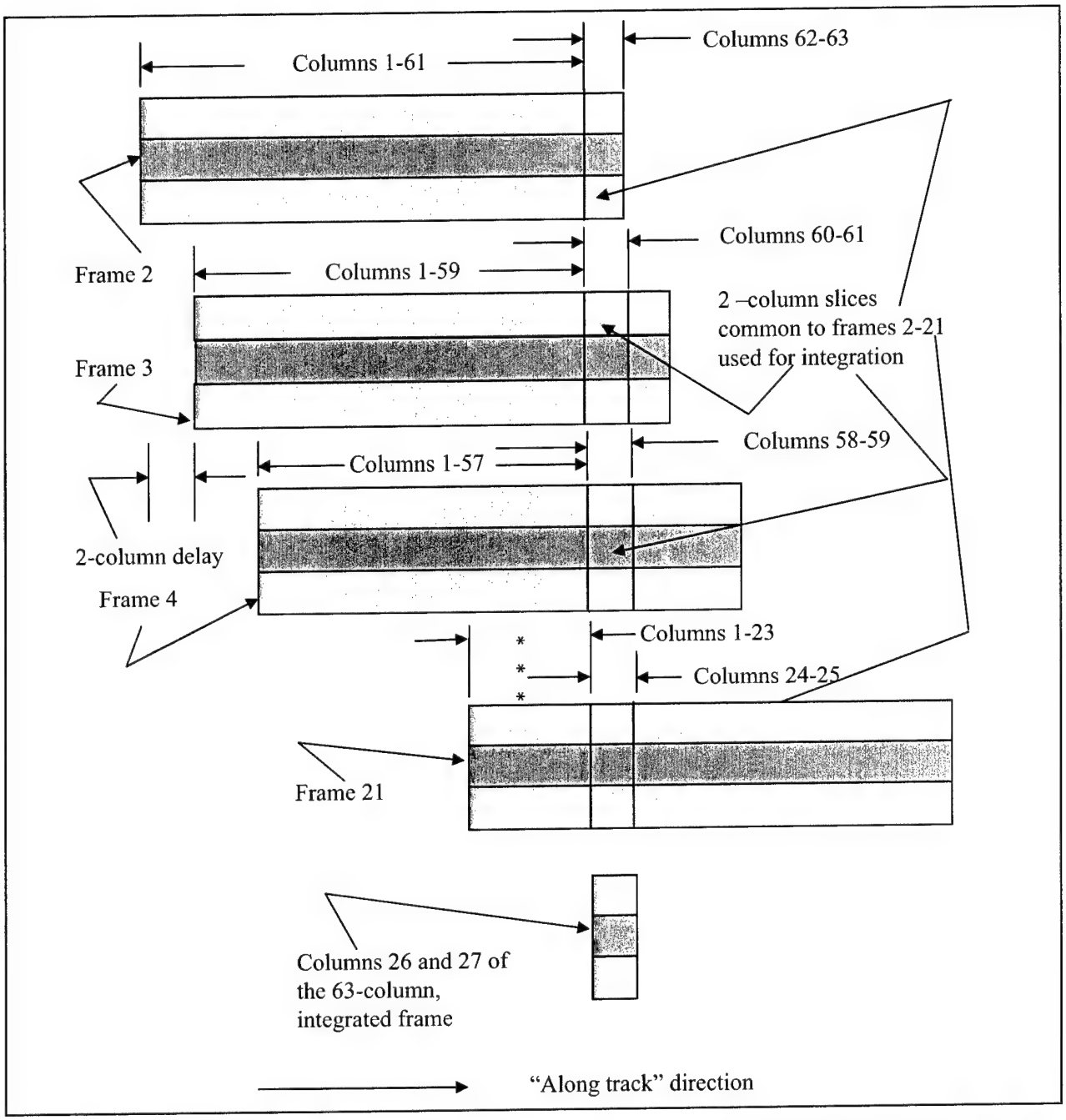


Figure 3. Formation of ***dx***(2)-column, integrated frame resulting from integrating 20 frames, where "column" refers to all pixels at the same "along track" position of the scene. This *dx*-column integrated frame results from the averaging of 20 independent brightness temperature measurements, contained in single frames 2–21, in each of the pixels ("cross track," "along track" locations) in columns 64 and 65 of the scene. These pixels are in columns 62 and 63 of single frame 2, columns 60 and 61 of single frame 3, columns 58 and 59 of single frame 4, and so on, down to columns 24 and 25 of single frame 21. These 20, 2-column, frame slices are averaged to form columns 26 and 27 of the 63-column, fully integrated frame being formed. Corresponding procedures are carried out to form the fully integrated frame's columns 28 and 29, 30 and 31, 32 and 33, and so on, down to columns 62 and 63.

### 3d. Formation of the fully integrated frame

Figure 4 shows how the processed, fully-integrated frame is formed. The first ***dx***(=2)-column integrated frame, which contains columns 26 and 27 of the fully integrated frame is concatenated to the end of the ***Com_cols*** (=25)-column partially integrated frame, which contains columns 1-25 of the fully integrated frame. Then the second ***dx***(=2)-column integrated frame, which contains columns 28 and 29 of the fully integrated frame, is concatenated to the end of the frame resulting from the previous concatenation. This concatenation procedure is repeated until all 63 columns of the fully integrated frame are formed.

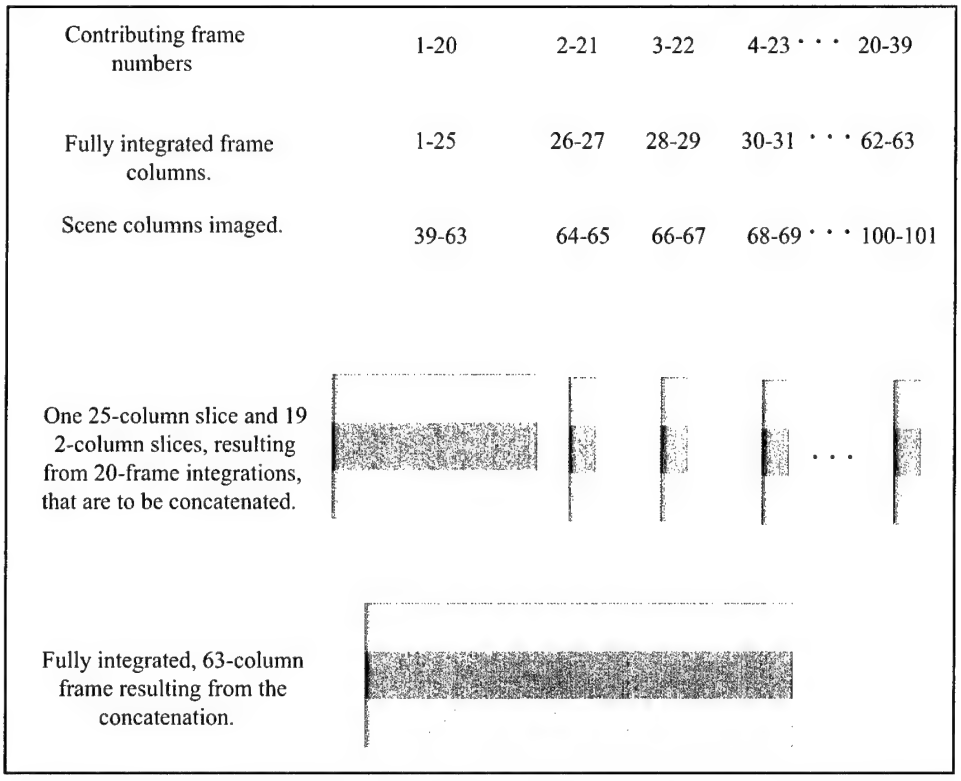


Figure 4. Concatenation of one, 25-column slice formed by integrating 25-column portions of frames 1–20, where "column" refers to all brightness temperature pixels at the same "along track" position of the scene, (see Figure 2), and 19, 2-column slices, each formed by integrating 2-column portions of frames 2–21, frames 3–22, frames 4–23, and so on, down to frames 20–39 (see Figure 3). The result is a fully integrated, 63-column frame.

It was seen in subsections 2b that the number of single frames required to form the partially integrated frame is ***Nframes,*** and it was seen in subsection 2c that the number of additional single frames required to form all the required ***dx***-column integrated frames is ***Nframes***-1. Thus, the total number of single frames, ***Nfull***, that need to be simulated for the formation of a fully integrated frame is

$$Nfull = 2(Nframes) - 1. \quad (5)$$

For ***Nframes*** = 20 equation 5 yields ***Nfull*** = 39.

Since there is a frame-to-frame delay of ***dx*** column pixels, the simulated scene must have at least ***Ncols_scene*** columns, where

$$Ncols_scene = Ncols + (Nfull-1)dx. \quad (6)$$

In our case, for which ***Ncols*** = 63, ***Nframes*** = 20, and ***dx*** = 2, equations 5 and 6 yield ***Ncols_scene*** = 139. This is the number of "along track" brightness temperature measurements that need to be made in the scene for each "cross-track" position to fully integrate all the pixels in each of the 63 columns of the sensor's FOV.

Clearly the maximum value, ***Nframes_max***, that ***Nframes*** may have when the column size of the frames is ***Ncols*** and the frame-to-frame column pixel delay is ***dx*** is

$$Nframes_max = \text{smallest}(Nframes_maxp, Nframes_maxd), \quad (7)$$

where smallest( ) indicates the smallest of the quantities in the parentheses. In our case, for which ***Ncols*** = 63 and ***dx***=2, equations 3, 4, and 7 yield ***Nframes_max*** = 31.

## 4. Simulation Steps

In summary, the steps of the simulation are as follows:

1. Given ***Nrows, Ncols*** and ***dx***, compute ***Nframes_maxp*** from equation 3 and ***Nframes_maxd*** from equation 4.

2. Choose a value of ***Nframes*** satisfying

$$1 < Nframes < Nframes_max, \quad (8)$$

where ***Nframes_max*** is computed from equation 7.

3. Simulate a scene having ***Nrows*** rows and at least ***Ncols_scene*** columns, where ***Ncols_scene*** is computed from equations 5 and 6.

4. Apply terrain variation noise to the scene, as discussed in Section 2b.

5. Form ***Nfull*** single frames based on the simulated scene, where ***Nfull*** is computed from equation 5.

6. Distort the brightness temperature profiles of each of the ***Nfull*** frames, as discussed in section 2c.

7. Add thermal noise to each of the ***Nfull*** frames, as discussed in section 2d.

8. In the manner discussed in section 3b form the partially integrated frame, having ***Nrows*** rows and ***Com_cols***, where the latter is computed from equation 2.

9. Form the ***Nframes*** − 1, ***dx***-column, integrated frames, as discussed in section 3c.

10. As discussed in subsection 3d, concatenate the partially integrated frame and the ***Nframes*** − 1, ***dx***-column, integrated frames to form the fully integrated frame.

# 5. Simulation Results

## 5a. Frame images and plots

Sections 3b and 3c described in detail how one ***com_cols***-column, partially integrated frame and several ***dx***-column integrated frames, respectively, may be generated from the simulated, single, image frames extracted from the scene by adding appropriate portions of some number of sets of ***Nframes*** consecutive frames. Figure 5 shows frames at three stages in the integration process. The road and vegetation growth average brightness temperatures are 270 K and 275 K, respectively ($\Delta T$ = 5 K), the terrain variation, standard deviation, ***mrtte***, is 1K, the thermal noise, standard deviation, ***mrtth***, is 10 K, and the psf is that of a PMMW imaging system at 84.5 GHz with a 58-cm diameter antenna, for which ***osamp*** = 2. Figure 5a shows a simulated, single, image frame, to which only terrain variation noise was added. The vegetation growth-to-road contrast in Figure 5a is quite good, since ***mrtte*** is small compared to $\Delta T$. Figure 5b shows the same frame after convolution with the psf was performed and thermal noise was added. The growth-to-road contrast in Figure 5b is poor since ***mrtth*** is larger than $\Delta T$, making it virtually impossible to discern the road from the vegetation growth. Figure 5c shows the processed, fully integrated frame arising from a 20-frame integration. It is seen that the integration has greatly improved the vegetation growth-to-road contrast over that of Figure 5b, to the extent that now the road and vegetation growth are easily distinguishable.

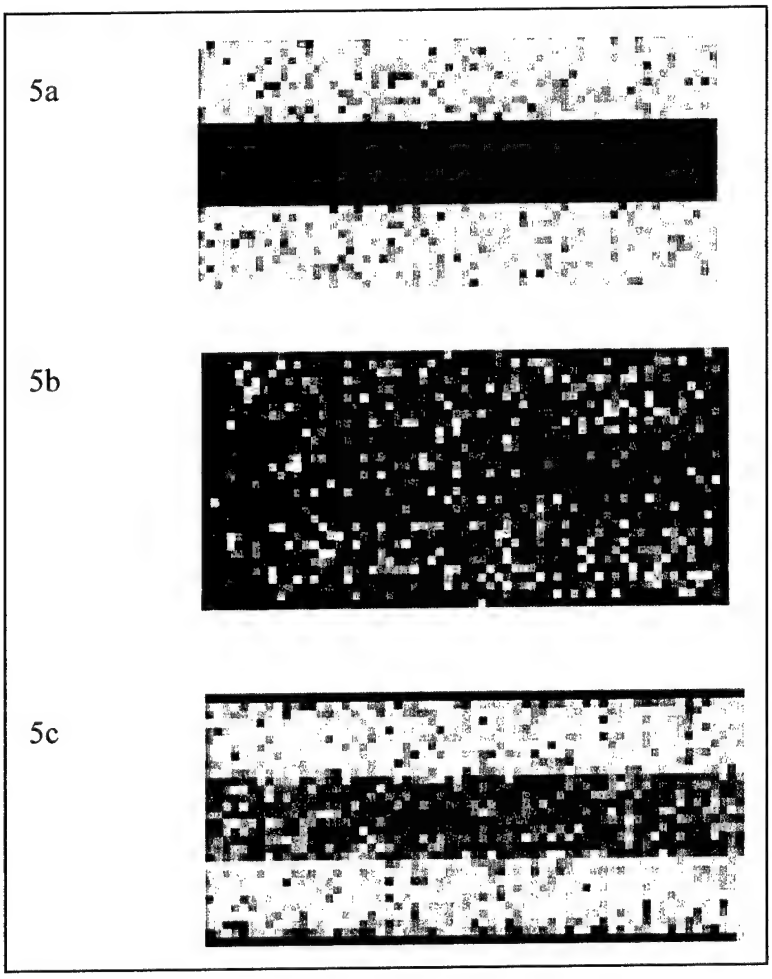


Figure 5. Images of a single and processed frame with a road (center patch) average brightness temperature of 270 K, a growth (upper and lower patches) average brightness temperature and a thermal noise minimum resolvable brightness temperature difference of 10 K. The psf is appropriate for a PMMW imaging system at 84.5 GHz oversampling the scene by ×2. 5a. A simulated, single frame that has terrain variation noise only. 5b. The simulated, single frame that results from convolving the frame in 5a with the psf and adding thermal noise. 5c. The fully integrated frame arising from the integration of 20 consecutive, single frames, such as the one in 5b, in the manner illustrated in Figures 1–4.

Figure 6 shows a plot of the brightness temperatures in column 32 vs. row number of column 32 for the images in Figures 5a(stars), 5b(circles), and 5c(squares). Note the scatter in both vegetation growth and road regions for the pixels of the single frame (circles) whose temperature profiles had terrain variation and thermal noise added, and on which convolution with psf was performed. That scatter is much greater than that of either the pixels of the same frame *prior* to psf distortion and thermal noise addition (stars), or the pixels of the processed, fully integrated frame resulting from a 20-frame integration (squares). The very low value and large deviation from the average of the brightness temperatures of the pixels of rows 1 and 30 seen both in Figure 5c as well as in the fully integrated frame plot (squares) of Figure 6 are edge effects due to the abrupt cutoff of brightness temperature where the vegetation growth strips end.

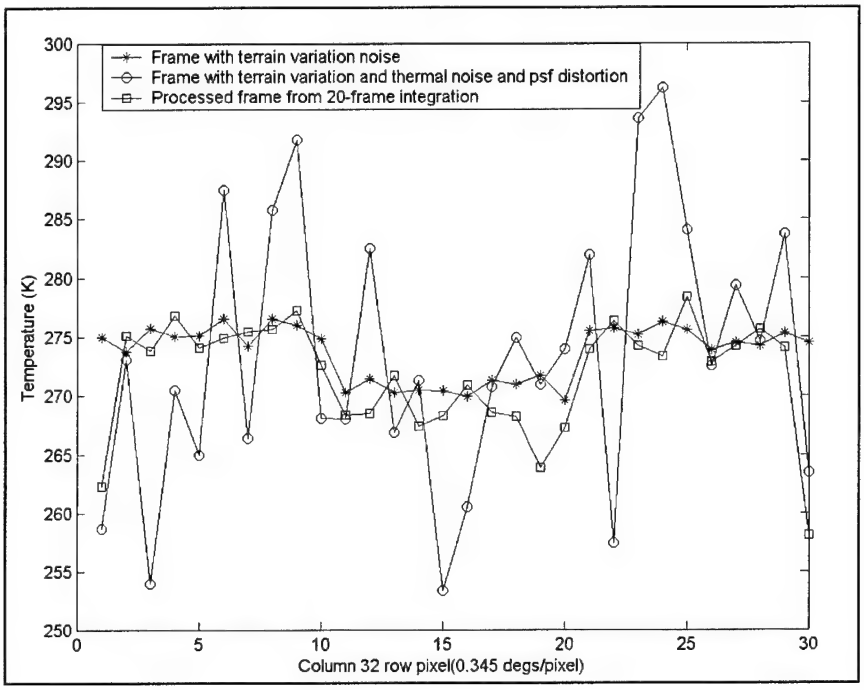


Figure 6. Plots of brightness temperature at "along track" position 32 vs. "cross track" position in a frame having only terrain variation, in a frame having both terrain variation and thermal noise, as well as distortion from the psf and the processed frame arising from the integration of 20 frames. The road average brightness temperature is 270 K, the growth average brightness temperature is 275 K, the terrain variation minimum resolvable brightness temperature difference is 1K, the thermal noise minimum resolvable brightness temperature difference is 10 K, and the psf is appropriate for a PMMW imaging system that oversamples the scene by ×2. The 20-frame integration processes illustrated in Figures 1–4.

## 5b. Contrast figure of merit

In this work the brightness temperature contrast figure of merit was taken to be the contrast-to-noise ratio, ***cnr***, in dB, defined as

$$\boldsymbol{cnr}(\mathrm{dB}) \equiv (10)\log(\Delta \boldsymbol{T}/\sigma_{\mathrm{all}}), \tag{9}$$

where $\boldsymbol{\Delta T}$ is the vegetation growth-to-road brightness temperature difference, and $\boldsymbol{\sigma}_{\mathrm{all}}$ is computed either from the simulated, fully integrated frame or by means of the central limit theorem.

In the simulations $\boldsymbol{\sigma}_{\mathrm{all}}$ was computed as the weighted average of the standard deviations, $\boldsymbol{\sigma}_{\mathrm{growth}}$ and $\boldsymbol{\sigma}_{\mathrm{road}}$ of the brightness temperatures in the vegetation growth and road areas, respectively, of the fully integrated frame. Thus $\boldsymbol{\sigma}_{\mathrm{all}}$ was computed as $\boldsymbol{\sigma}_{\mathrm{sim}}$, where

$$\sigma_{sim} = (2/3)\sigma_{growth} + (1/3)\sigma_{road}, \tag{10}$$

since there are twice as many vegetation growth pixels as road pixels in a frame.

In the absence of distortion due to the psf the value of $\sigma_{all}$ can still be computed from the fully integrated frame using Equation 10. However $\sigma_{all}$ can also be predicted using the Central Limit Theorem *(6)* (CLT). That theorem states that if $x$ and $y$ are completely independent variables, and have distributions with variances, $\sigma_x^2$ and $\sigma_y^2$, then the variance, $\sigma^2$, of the distribution of $x + y$ values is

$$\sigma^2 = \sigma_x^2 + \sigma_y^2. \tag{11}$$

Each integrated frame pixel has a temperature deviation from 270 K or from 270 + $\Delta T$ due to terrain variation noise, characterized by ***mrtte***, and thermal noise characterized by ***mrtth***. Since the terrain variation noise and thermal noise are completely independent, from equation 11 the variance, $\sigma_{CLT}^2$, of the integrated frame can be written as having two independent contributions, one from the terrain noise and one from the thermal noise:

$$\sigma_{CLT}^2 = \sigma_1^2(mrtte) + \sigma_2^2(mrtth), \tag{12}$$

where $\sigma_1^2(mrtte)$ and $\sigma_2^2(mrtth)$ are functions of ***mrtte*** and ***mrtth,*** respectively. But the temperature deviation of any fully integrated frame pixel due to the terrain variation noise arises from the addition of ***Nframes*** pixels, each of which has the *same* member of a zero-mean, brightness temperature distribution whose variance is $(mrtte)^2$. Therefore

$$\sigma_1^2(mrtte) = (mrtte)^2. \tag{13}$$

On the other hand, the temperature deviation of an integrated frame pixel due to thermal noise arises from the addition of ***Nframes*** pixels, each of which has a *different* member of a zero-mean, brightness temperature distribution whose variance is $(mrtth)^2$. For that situation it can be shown *(6)* that the CLT gives

$$\sigma_2^2(mrtth) = \frac{(mrtth)^2}{Nframes}. \tag{14}$$

Equations (12) thru (14) therefore yield a CLT-based value for $\sigma_{all}$ of $\sigma_{CLT}$, where

$$\sigma_{CLT} = \left[(mrtte)^2 + \frac{(mrtth)^2}{Nframes}\right]^{1/2}. \tag{15}$$

Figures 7, 8, 9, and 10 compare plots of ***cnr*** vs. ***Nframes***, as computed from equation 9 for $\Delta T$ =5 K, ***mrtte*** = 1 K, and ***mrtth***=3 K, 5 K, 10K, and 15 K, respectively. The psf is that of a sensor frequency of 84.5 GHz and an antenna diameter of 58 cm, for which ***osamp*** = 2 when the pixel angle is 0.38 deg. For the solid curve in each figure $\sigma_{all}$ in equation 9 was taken to be $\sigma_{CLT}$ computed according to equation 15; for the circles curve in each figure $\sigma_{all}$ in equation 9 was taken to be $\sigma_{sim}$ computed according to equation 10 without distortion from the psf; and for the asterisks curve in each figure $\sigma_{all}$ in equation 9 was taken to be $\sigma_{sim}$ computed according to

equation 10 with distortion from a psf . As expected the agreement between the circles and the solid curve is excellent. Figures 7, 8, 9, and 10 show that, whether or not distortion is included in the simulation, ***cnr*** increases monotonically with ***Nframes***. However, unlike the shape of the ***cnr*** data without blurring, which is always concave looking from lower toward higher dB, the ***cnr*** data with blurring starts out concave, but it transitions to convex at ***Nframes*** values between 15 and 20. They also show that for a given value of ***Nframes*** the reduction in ***cnr*** with distortion from its value without distortion is a decreasing function of ***mrtth***.

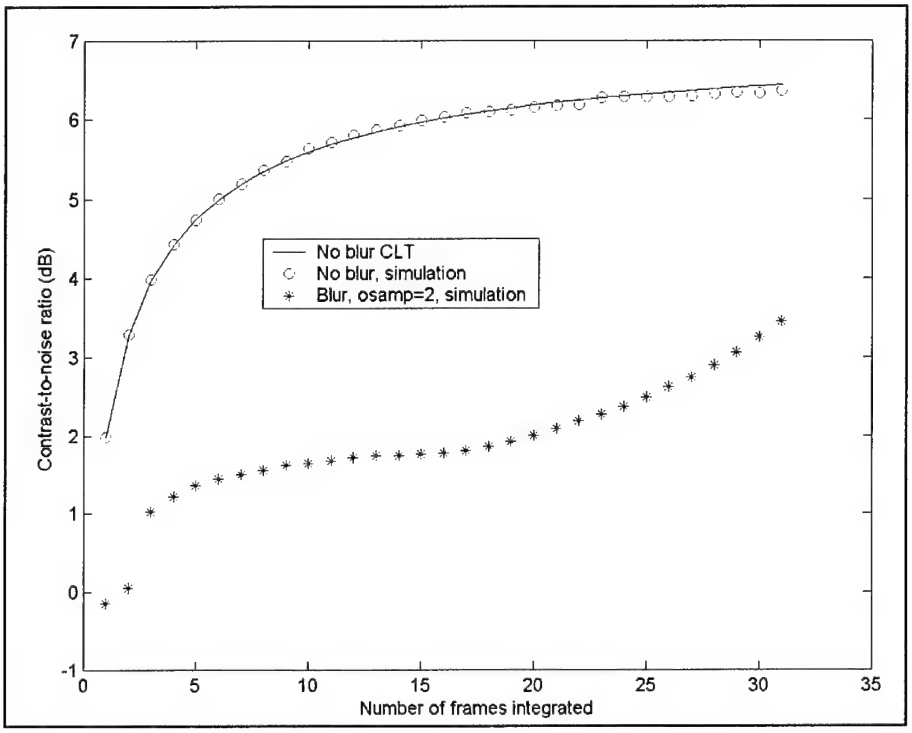


Figure 7. Contrast-to-noise ratio vs. number of frames integrated for the fully integrated frame based on the central limit theorem (CLT), and as generated by simulations with blurring by a point spread function for an oversampling of ×2, and without blurring. The vegetation growth-to-road brightness temperature difference is 5 K, the terrain variation minimum resolvable brightness temperature difference is 1 K, and the thermal noise minimum resolvable brightness temperature difference is 3 K.

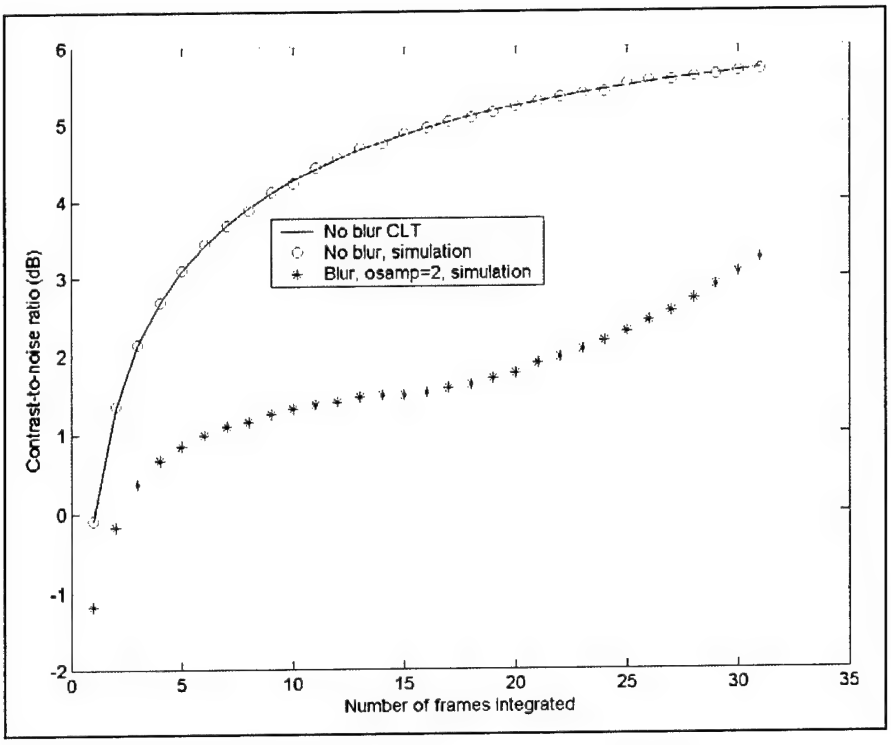


Figure 8. Contrast-to-noise ratio vs. number of frames integrated for the fully integrated frame based on the central limit theorem (CLT), and as generated by simulations with blurring by a point spread function for an oversampling of ×2, and without blurring. The vegetation growth-to-road brightness temperature difference is 5 K, the terrain variation minimum resolvable brightness temperature difference is 1 K, and the thermal noise minimum resolvable brightness temperature difference is 5 K.

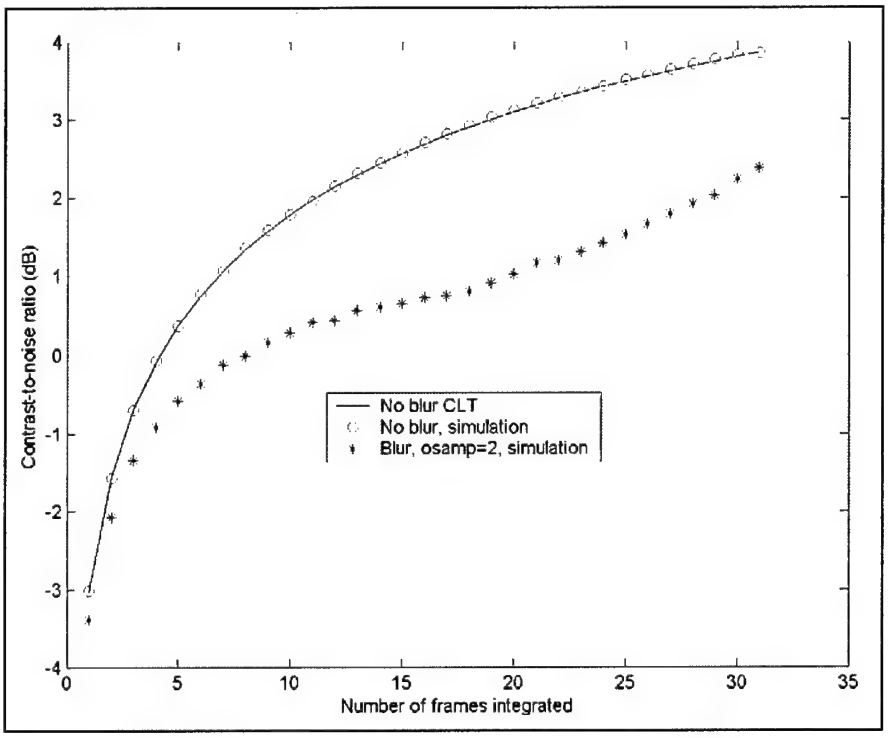


Figure 9. Contrast-to-noise ratio vs. number of frames integrated for the fully integrated frame based on the central limit theorem (CLT), and as generated by simulations with blurring by a point spread function for an oversampling of ×2, and without blurring. The vegetation growth-to-road brightness temperature difference is 5 K, the terrain variation minimum resolvable brightness temperature difference is 1 K, and the thermal noise minimum resolvable brightness temperature difference is 10 K.

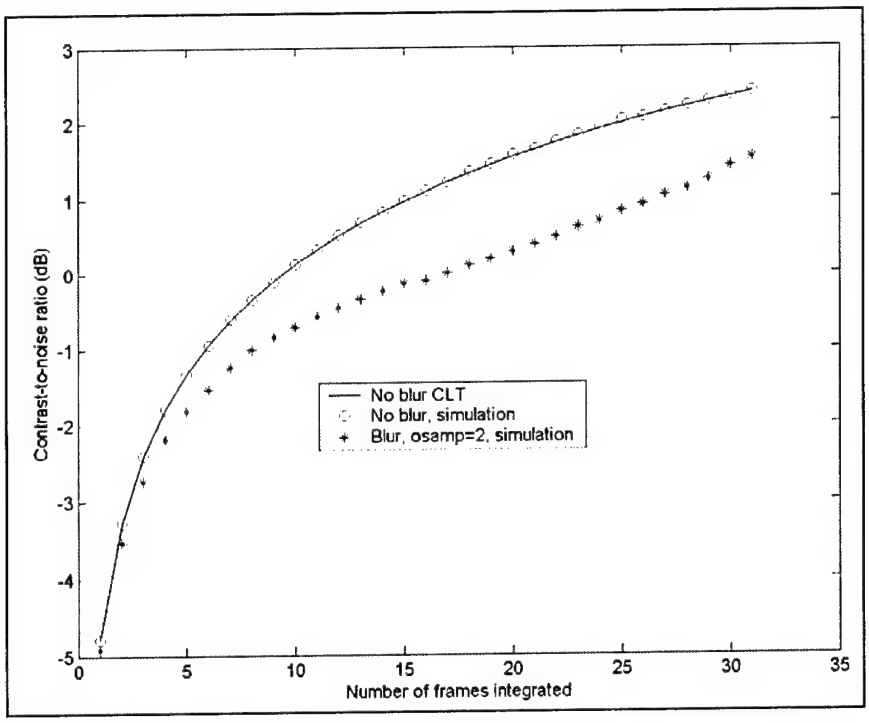


Figure 10. Contrast-to-noise ratio vs. number of frames integrated for the fully integrated frame based on the central limit theorem (CLT), and as generated by simulations with blurring by a point spread function for an oversampling of ×2, and without blurring. The vegetation growth-to-road brightness temperature difference is 5 K, the terrain variation minimum resolvable brightness temperature difference is 1 K, and the thermal noise minimum resolvable brightness temperature difference is 15 K.

Figure 11 compares plots of ***cnr*** vs. ***Nframes***, as computed from equation 9 for $\Delta T = 5$ K, ***mrtte*** = 1 K, and ***mrtth*** = 5 K. For the solid curve $\sigma_{all}$ in equation 9 was taken to be $\sigma_{CLT}$ computed according to equation 15; for the circles curve $\sigma_{all}$ in equation 9 was taken to be $\sigma_{sim}$ computed according to equation 10 without distortion from a psf; for the squares curve, the asterisks curve, and for the plusses curve $\sigma_{all}$ in equation 9 was taken to be $\sigma_{sim}$ computed according to equation 10 with distortion from a psf for which the sensor frequency is 84.5 GHz and the antenna aperture diameter is 116 cm, 58 cm, and 29 cm, respectively, for which ***osamp*** = 1, 2, and 4, respectively (see equation 1), when the pixel angle of 0.38 deg. It was already seen in Figures 7, 8, 9, and 10 that there is excellent agreement between ***cnr*** values for no blurring calculated using $\sigma_{sim}$ and ***cnr*** values based on $\sigma_{CLT}$. Figure 11, however, shows that, at any given value of ***Nframes*** the ***cnr*** data based on $\sigma_{sim}$ increases with decreasing ***osamp***, and it approaches the maximum ***cnr*** value, which is the one based on $\sigma_{CLT}$, as ***osamp*** approaches 1. The reason this occurs may be seen from the definition of ***osamp*** in equation 1. As the null-to-null angle of the psf approaches the pixel angle from above, so that ***osamp*** approaches 1 from above, the psf, as a function of angle, *in units of the pixel angle*, in both the "cross track" and "along track" directions, approaches a delta function in both of those arguments. Therefore, since the convolution of any function with a delta function has no effect at all on the shape of the function, the image in a frame suffers practically no distortion at all when it is convolved with a psf for

***osamp*** =1. The important conclusion from Figure 11 is that increasing ***Nframes*** is not the only way to increase ***cnr***. It may also be increased from its value for some ***Nframes*** and pixel angle by increasing the sensor's antenna aperture at a given frequency, which results in decreasing the null-to-null angle, and, therefore, according to equation 1, in decreasing ***osamp***. That method of increasing ***cnr*** may be the preferred one since it minimizes the computational effort required to perform the frame integration. However, at the present time 58 cm is the practical upper limit on the diameter of a PMMW sensor that can be accommodated by a low-flying aircraft that is suitable for road navigation.

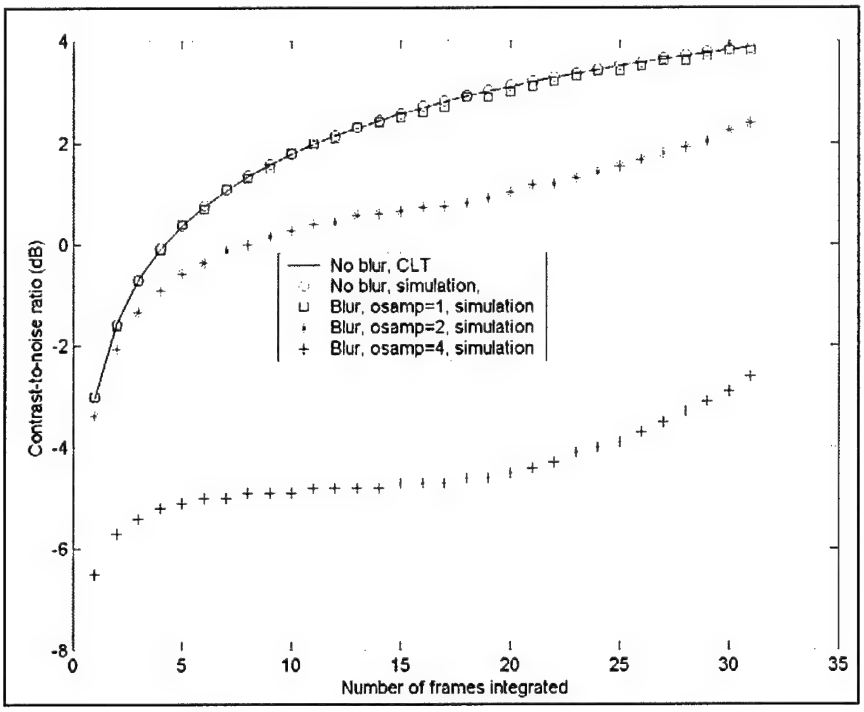


Figure 11. Brightness temperature contrast-to-noise ratio vs. number of frames integrated for the fully integrated frame based on the central limit theorem (CLT), and as generated by simulations without blurring as well as with blurring by point spread functions for oversamplings of ×1 (aperture diameter = 116 cm), ×2 (aperture diameter = 58 cm), and ×4 (aperture diameter = 29 cm). The vegetation growth-to-road brightness temperature difference is 5 K, the terrain variation minimum resolvable brightness temperature difference is 1 K, and the thermal noise minimum resolvable brightness temperature difference is 10 K.

## 5c. Road distinguishability

All three images in Figures 12a, 12b, and 12c are for $\Delta T$ = 5 K, ***mrtte*** =1 K, ***mrtth*** =10 K. Just as for the data in Figures 5–10, the psf for the data in Figures 12a, 12b, and 12c is that of a sensor frequency of 84.5 GHz and a sensor antenna aperture of 58 cm, which gives rise to ***osamp*** = 2 when the pixel angle is 0.86 deg. The values of ***Nframes*** in Figures 12a, 12b, and 12c are 8, 20, and 29, respectively, which, as is seen in Figure 9, give rise to ***cnr*** values of 0 dB, 1 dB, and 2 dB, respectively. Visually distinguishing the road in Figure 12a would be difficult. Visually distinguishing it in Figure 12b would be feasible almost over the entire length of the road, and

visually distinguishing it in Figure 12c is definitely feasible along the entire length of the road. For a given frequency, antenna diameter, and pixel angle, i.e., a given ***osamp***, the degree of visual distinguish ability of the road as a function of the ***cnr*** resulting from frame integration was the same for all combinations of values of $\Delta T$, ***mrtte***, and ***mrtth*** for which simulations were carried out.

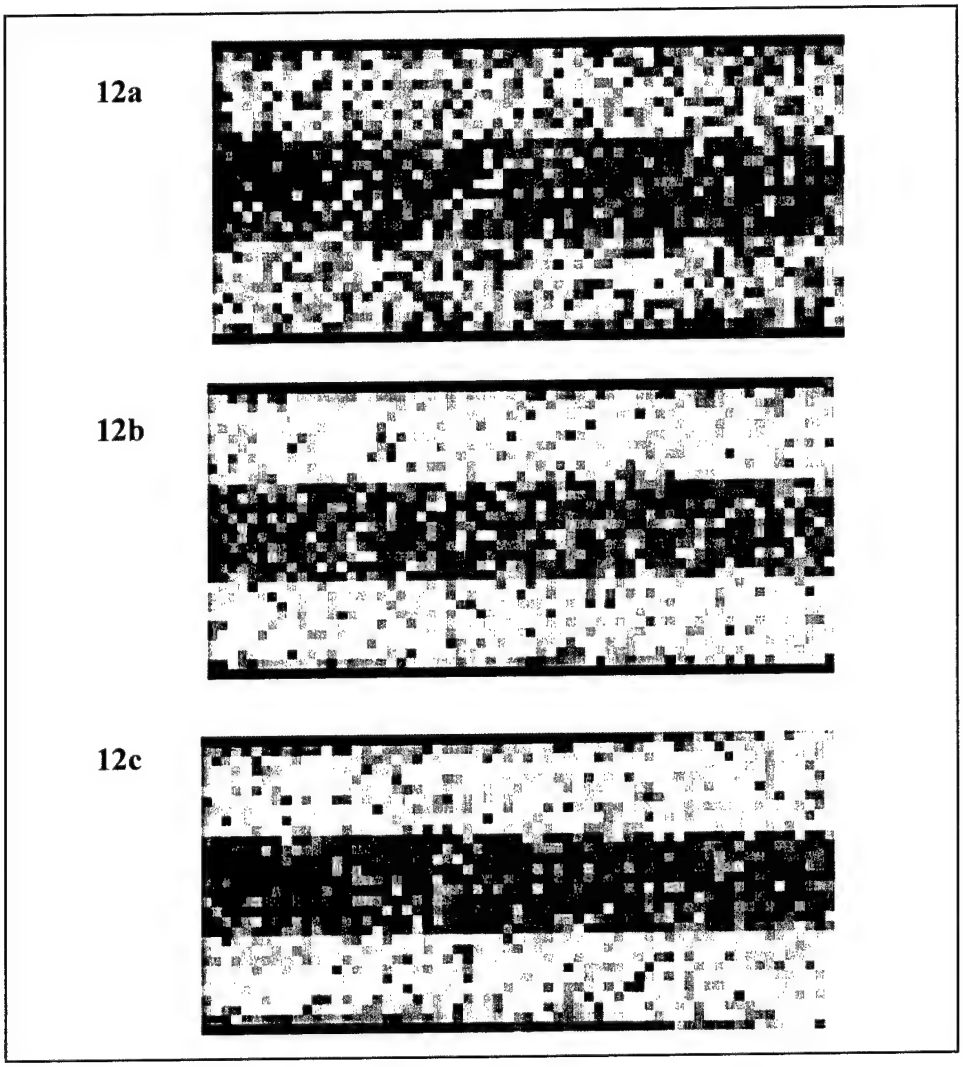


Figure 12. Fully integrated frames resulting in brightness temperature contrast-to-noise ratios of 0 dB (12a), 1 dB (12b), and 2 dB (12c) for a vegetation growth-to-road brightness temperature difference of 5 K, a terrain variation minimum resolvable brightness temperature difference of 1 K, and a thermal noise minimum resolvable brightness temperature difference of 0 K.

Tables 2a, 2b, 2c, and 2d give, for each set of the values of $\Delta T$, ***mrtte***, and ***mrtth*** that were studied, the smallest value of ***Nframes*** for which ***cn r*** $\geq$ 0 dB, the smallest value of ***Nframes*** for which ***cnr*** $\geq$ 1 dB, and the smallest value of ***Nframes*** for which ***cnr*** $\geq$ 2 dB. Table 2a shows that for $\Delta T$ =1 K, even for values of ***mrtte*** and ***mrtth*** as small as 0 K and 3 K, respectively, and for $\Delta T$ =2 K, even for those values as small as 0 K and 5 K, respectively, that even after integrating 31 frames the resulting ***cnr*** was less than 0 dB. Noted that 31 is the largest possible number of frames, ***Nframes_max*** (see equation 7), that can be integrated for a fully integrated frame in this case. Only for $\Delta T$ =2 K, ***mrtte*** = 0 K, and ***mrtth*** = 3 K and only after integrating 31 frames is ***cnr*** $\geq$ 0 dB. Table 2b shows that, for $\Delta T$=5 K, a ***cnr*** $\geq$ 2 dB can be achieved for all combinations of the values of ***mrtte*** and ***mrtth*** studied, except 1 K and 15 K, respectively, 2 K and 10 K, respectively, and 2 K and 15 K, respectively, for which the maximum attainable ***cnr*** was between 1 dB and 2 dB. Tables 2c and 2d show that for $\Delta T$ = 10 K and 15 K, respectively, ***cnr*** $\geq$ 2 dB is attainable for all values of combinations of the values of ***mrtte*** and ***mrtth*** studied.

Table 2a. Minimum required number of frames that must be integrated to achieve specified values of contrast-to-noise ratio (*cnr)* for vegetation growth-to-road brightness temperature differences of 1 K and 2 K.

| **Vegetation growth-to-road brightness temperature difference (K)** | **Terrain mean resolvable brightness temperature (K)** | **Thermal mean resolvable brightness temperature (K)** | **Minimum number of frames to integrate for *cnr* ≥ 0 dB** | **Minimum number of frames to integrate for *cnr* ≥ 1 dB** | **Minimum number of frames to integrate for *cnr* ≥ 2 dB** |
|---|---|---|---|---|---|
| 1 | 0,1,2 | 3,5,10,15 | >31 | >31 | >31 |
| 2 | 0 | 3 | 31 | >31 | >31 |
| 2 | 0 | 5,10,15 | >31 | >31 | >31 |
| 2 | 1,2 | 3,5,10,15 | >31 | >31 | >31 |

Table 2b. Minimum required number of frames that must be integrated to achieve specified values of contrast-to-noise ratio (*cnr*) for a vegetation growth-to-road brightness temperature difference of 5 K.

| Vegetation growth-to-road brightness temperature difference (K) | Terrain mean resolvable brightness temperature (K) | Thermal mean resolvable brightness temperature (K) | Minimum number of frames to integrate for *cnr* ≥ 0 dB | Minimum number of frames to integrate for *cnr* ≥ 1 dB | Minimum number of frames to integrate for *cnr* ≥ 2 dB |
|---|---|---|---|---|---|
| 5 | 0 | 3 | 2 | 3 | 5 |
| 5 | 0 | 5 | 3 | 6 | 21 |
| 5 | 0 | 10 | 8 | 19 | 27 |
| 5 | 0 | 15 | 17 | 26 | >31 |
| 5 | 1 | 3 | 2 | 3 | 20 |
| 5 | 1 | 5 | 3 | 7 | 23 |
| 5 | 1 | 10 | 8 | 20 | 29 |
| 5 | 1 | 15 | 17 | 27 | >31 |
| 5 | 2 | 3 | 2 | 6 | 27 |
| 5 | 2 | 5 | 3 | 15 | 30 |
| 5 | 2 | 10 | 10 | 25 | >31 |
| 5 | 2 | 15 | 21 | 31 | >31 |

Table 2c. Minimum required number of frames that must be integrated to achieve specified values of contrast-to-noise ratio (*cnr*) for a vegetation growth-to-road brightness temperature difference of 10 K.

| Vegetation growth-to-road brightness temperature difference (K) | Terrain mean resolvable brightness temperature (K) | Thermal mean resolvable brightness temperature (K) | Minimum number of frames to integrate for *cnr* ≥ 0 dB | Minimum number of frames to integrate for *cnr* ≥ 1 dB | Minimum number of frames to integrate for *cnr* ≥ 2 dB |
|---|---|---|---|---|---|
| 10 | 0 | 3 | 1 | 1 | 1 |
| 10 | 0 | 5 | 1 | 1 | 2 |
| 10 | 0 | 10 | 2 | 3 | 4 |
| 10 | 0 | 15 | 3 | 5 | 9 |
| 10 | 1 | 3 | 1 | 1 | 1 |
| 10 | 1 | 5 | 1 | 1 | 2 |
| 10 | 1 | 10 | 2 | 3 | 4 |
| 10 | 1 | 15 | 3 | 5 | 9 |
| 10 | 2 | 3 | 1 | 1 | 1 |
| 10 | 2 | 5 | 1 | 1 | 2 |
| 10 | 2 | 10 | 2 | 3 | 5 |
| 10 | 2 | 15 | 3 | 5 | 9 |

Table 2d. Minimum required number of frames that must be integrated to achieve specified values of contrast-to-noise ratio (*cnr*) for a vegetation growth-to-road brightness temperature difference of 15 K.

| Vegetation growth-to-road brightness temperature difference (K) | Terrain mean resolvable brightness temperature (K) | Thermal mean resolvable brightness temperature (K) | Minimum number of frames to integrate for $cnr \geq 0$ dB | Minimum number of frames to integrate for $cnr \geq 1$ dB | Minimum number of frames to integrate for $cnr \geq 2$ dB |
|---|---|---|---|---|---|
| 15 | 0 | 3 | 1 | 1 | 1 |
| 15 | 0 | 5 | 1 | 1 | 1 |
| 15 | 0 | 10 | 1 | 1 | 2 |
| 15 | 0 | 15 | 2 | 2 | 3 |
| 15 | 1 | 3 | 1 | 1 | 1 |
| 15 | 1 | 5 | 1 | 1 | 1 |
| 15 | 1 | 10 | 1 | 1 | 2 |
| 15 | 1 | 15 | 2 | 2 | 3 |
| 15 | 2 | 3 | 2 | 5 | 27 |
| 15 | 2 | 5 | 1 | 1 | 1 |
| 15 | 2 | 10 | 1 | 1 | 2 |
| 15 | 2 | 15 | 2 | 2 | 4 |

## 6. Generation of Video Frames

As discussed in subsections 3b, 3c, and 3d, and as noted in Figure 4, adding the brightness temperature values in the pixels of appropriate columns of frame Nos. 1 thru 2(***Nframes***)–1 yields a processed image of scene columns Nos. (***Nframes***−1)***dx***+1 thru ***Ncols*** + (***Nframes***−1)***dx***. An analysis of the relationship between the portion of the scene from which some succeeding group of 2(***Nframes***)−1 unprocessed frames comes and the portion of the scene that is imaged by integrations involving that group of frames yields the following result: Let a fully, integrated frame be constructed, in the manner described in sections 3b, 3c, and 3d, from the 2(***Nframes***)−1 consecutive, unprocessed frames Nos.

$$(\boldsymbol{k}-1)\boldsymbol{N}+1 \text{ thru } (\boldsymbol{k}-1)\boldsymbol{N}+2(\boldsymbol{Nframes})-1, \tag{16a}$$

where ***k,*** the fully integrated frame number, can have the values

$$\boldsymbol{k} = 2,3,4\ldots, \tag{16b}$$

and,

$$\boldsymbol{N} = \text{floor}(\boldsymbol{Ncols/dx}). \tag{16c}$$

Then the scene columns imaged will be Nos.

$$(\boldsymbol{k}-1)\boldsymbol{Ncols}+(\boldsymbol{Nframes}-1)\boldsymbol{dx}+1-\boldsymbol{R} \text{ thru } (\boldsymbol{k})\boldsymbol{Ncols}+(\boldsymbol{Nframes}-1)\boldsymbol{dx}-\boldsymbol{R}, \tag{17a}$$

where ***R*** is the integer remainder

$$\boldsymbol{R} \equiv (\boldsymbol{Ncols}) \bmod(\boldsymbol{dx}) . \tag{17b}$$

Equations 16 and 17 show that for consecutives values of $\boldsymbol{k}$ for $\boldsymbol{k} \geq 2$ there is always overlap in the range of single frame Nos. of the ($\boldsymbol{Nframes}$)–1 single frames, but there is no overlap in the *scene columns* imaged by integrations of those frames. Table 3 shows that to be the case for our example of $\boldsymbol{Ncols}$=63, $\boldsymbol{Nframes}$=20, and $\boldsymbol{dx}$=2 for fully integrated frame numbers 2 or greater.

It is to be noted that Table 3 lists the scene columns imaged by the first fully integrated frame as 39 thru 101, consistent with Figure 4, for the values of $\boldsymbol{Ncols}$, $\boldsymbol{Nframes}$, and $\boldsymbol{dx}$ being considered. Thus, in this case there is a one-column overlap between the columns imaged by fully integrated frames 1 and 2. However, if a $\boldsymbol{k}$ of 1 and the values of the other parameters being considered here are substituted into equation 17a it gives the range of scene columns imaged by integrated frame No. 1 as 38 thru 100, which is incorrect. That is why equation 17a is only correct for $\boldsymbol{k} \geq 2$. It turns out, however, that if $\boldsymbol{Ncols}$ is an integral multiple of $\boldsymbol{dx}$, then, equation 17a does give the correct range of scene columns imaged by the fully integrated frame for all $\boldsymbol{k}$. In particular, the non-overlapping and consecutive ranges yielded by equation 17a for the scene columns imaged by the first ($\boldsymbol{k}$ =1) and second ($\boldsymbol{k}$=2) fully integrated frames are correct.

Table 3. Range of the frame numbers of the 39, consecutive single frames involved in forming each of the first 10, fully integrated frames. The fully integrated frames are formed by integrating portions of 20 consecutive, single frames from among those 39 consecutive, single frames. For each fully integrated frame number the table also gives the range of the column numbers of the scene columns imaged by those fully integrated frames. The number of columns in both the single and fully integrated frames is 63, and the frame-to-frame delay in "along track" brightness temperature pixels is 2.

| Processed, fully integrated frame No. | First single frame No. | 39th single frame No. | First scene column No. imaged | 63rd scene column No. imaged |
|---|---|---|---|---|
| 1 | 1 | 39 | 39 | 101 |
| 2 | 32 | 70 | 101 | 163 |
| 3 | 63 | 101 | 164 | 226 |
| 4 | 94 | 132 | 227 | 289 |
| 5 | 125 | 163 | 290 | 352 |
| 6 | 156 | 194 | 353 | 415 |
| 7 | 187 | 225 | 416 | 478 |
| 8 | 218 | 256 | 479 | 541 |
| 9 | 247 | 287 | 542 | 604 |
| 10 | 280 | 318 | 605 | 667 |

As was stated in Section 2b, the unprocessed frame rate upon which the value 2 for the frame-to-frame delay in "along track" pixels, $\boldsymbol{dx}$, is based is 30 Hz. It is important that the actual navigating video processing system maintain that rate as closely as possible. Therefore, the simulations performed in this work, besides yielding the processed frames themselves, also timed the frame integration process. Those timing results imply very high rates, on the order of 150 Hz. Thus, maintaining a desired, smaller video rate, such as 30 Hz, with this type of processing should be quite feasible.

## 7. Conclusions

Simulations were carried out of the generation of passive millimeter-wave (PMMW) digital video images of a simple road scene by a PMMW imaging system mounted on a moving aircraft. The simulations employed documented measurements of mean millimeter-wave (MMW) brightness temperatures and minimum resolvable temperatures for various terrains. The resolution spot size, frame rate, and sampling frequency assumed for the simulations are those for an 84.5-GHz imaging system under development. Measurements with PMMW imaging systems have shown that road and vegetation growth mean brightness temperatures can differ by an amount so small as to make it comparable to the minimum resolvable temperature *(1,4)*. A single image frame resulting from simulating such a scene was found to have insufficient contrast for visually distinguishing the road from the growth. However, processed frames formed by integrating some number of consecutive video frames had sufficient contrast to enable one to visually distinguish the road from its surroundings and allow for reliable navigation. It was found that a ***cnr*** value of only 2 dB was necessary to enable completely reliable visual vegetation-growth-to-road distinction.

For average vegetation-growth-to-road temperatures differences $\Delta T$ = 1 K or 2 K it was not possible to attain ***cnr*** $\geq$ 1 dB needed for reliable visual distinction of the vegetation growth and the road for any combination of the values of the minimum resolvable temperatures due to terrain variations, ***mrtte***, of 0 K, 1 K, or 2 K, and the values of minimum resolvable temperatures due to thermal noise, ***mrtth***, 3 K, 5 K, 10 K, or 15 K. However, for an average vegetation-growth-to-road temperatures differences $\Delta T$ = 5 K, 10 K, or 15 K it was possible to attain the ***cnr*** $\geq$ 1 dB for all of the combinations of ***mttte*** and ***mrtth***, and ***cnr*** $\geq$ 2 dB for most of the combinations of ***mrtte*** and ***mrtth***.

The ***cnr*** of processed frames arising from the simulations was found to increase monotonically, although not linearly, as a function of the number of frames integrated. The diameter of the PMMW imaging system assumed in most of the simulations performed is 58 cm. This is the current state-of-the-art maximum diameter for such a system mounted on a low-flying aircraft. It was found that if this antenna aperture size could be doubled to 116 cm, the resulting contrast-to-noise ratio for any given number of frames integrated could attain the maximum ***cnr*** that is predicted by the central limit theorem. In this manner one can reduce the number of frames that need to be integrated to attain the ***cnr*** required for reliable road navigation, while minimizing the computational effort needed for the integration process.

A number of important effects, such as the dependence of measured terrain brightness temperature on depression angle from nadir to zenith, and frame-to-frame registration have not been included in these simulations. Nevertheless, the results of these simulations imply that a state-of-the-art, PMMW, imaging system employing simple, video frame integration holds out the promise of enabling road navigation at modest altitudes and non-ideal atmospheric conditions. In addition, results of timing the frame integration steps indicate that desired video frame rates can be easily maintained for the processed frames.

## References


1. Wilson, W.J.; Howard, R.J.; Ibbott, A.C.; G.S. Parks, G.S.; W.R. Ricketts, W.R. "Millimeter-Wave Imaging Sensors," pp 1026-1035, *IEEE Trans. On Microwaves Theory & Techniques,* MTT-34, No. 10, October 1986, and Wilson, W. J.: Ibbott, A. C. "Millimeter-Wave Imaging Sensor Data Evaluation", Jet Propulsion Lab Pub. 87-16, California Institute of Technology, May 1987.

2. Silverstein, J. "Passive Millimeter-Wave Image Resolution Improvement by Linear and Non-linear Algorithms", *Proc. SPIE, Passive Millimeter-Wave Imaging Technology V*, R. M. Smith and R. Appleby, eds., April 2001, pp 132-153.

3. Martin, C.; Clark, S. E.; Lovberg, J. A.; Galliano, J. A. "Real-Time Passive Millimeter-Wave Imaging From a Helicopter Platform", *Proc. SPIE, Infrared and Passive Millimeter-Wave Imaging Systems: Design, Analysis, Modeling, and Testing,* Smith R. M.; Appleby, R. eds., April 2000 pp 22-29.

4. Nemarich, J.; Cassidy, T. W. "Passive Millimeter-Wave Imaging for Detection of Military Vehicles From Airborne Platforms," *Proc. 4th Int'l MSS*, 45, No. 2, Sep. 2000, pp 17-34.

5. Silverstein, J. D. "Resolution and Resolution Improvement of Passive Millimeter-Wave Images", *Proc. SPIE, Passive Millimeter-Wave Imaging Technology III,* R. M. Smith, ed., April 1999, pp 140-154.

6. Barlow, R. J. "Statistics, chapter 4, John Wiley, 1989